Inorganic Chemistry

Article

pubs.acs.org/IC

Stable Luminescent Metal–Organic Frameworks as Dual-Functional Materials To Encapsulate Ln^{3+} Ions for White-Light Emission and To Detect Nitroaromatic Explosives

Wei Xie,[†] Shu-Ran Zhang,[†] Dong-Ying Du,[†] Jun-Sheng Qin,[†] Shao-Juan Bao,[†] Jing Li,[†] Zhong-Min Su,*[,†] Wen-Wen He,[†] Qiang Fu,*[,†] and Ya-Qian Lan*[,†,‡]

[†]Institute of Functional Material Chemistry, Faculty of Chemistry, Northeast Normal University, Changchun 130024, Jilin, P. R. China

[‡]Jiangsu Key Laboratory of Biofunctional Materials, College of Chemistry and Materials Science, Nanjing Normal University, Nanjing 210023, Jiangsu, P. R. China

Supporting Information

ABSTRACT: A stable porous carbazole-based luminescent metal–organic framework, **NENU-522**, was successfully constructed. It is extremely stable in air and acidic/basic aqueous solutions, which provides the strategy for luminescent material encapsulation of Ln^{3+} ions with tunable luminescence for application in light emission. More importantly, **Ln^{3+}@NENU-522** can emit white light by encapsulating different molar ratios of Eu^{3+} and Tb^{3+} ions. Additionally, **Tb^{3+}@NENU-522** is found to be useful as a fluorescent indicator for the qualitative and quantitative detection of nitroaromatic explosives with different numbers of $-NO_2$ groups, and the concentrations of complete quenching are about 2000, 1000, and 80 ppm for nitrobenzene, 1,3-dinitrobenzene, and 2,4,6-trinitrophenol, respectively. Meanwhile, **Tb^{3+}@NENU-522** displays high selectivity and recyclability in the detection of nitroaromatic explosives.

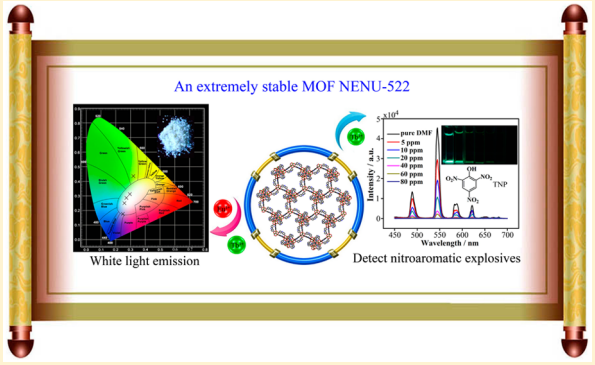

INTRODUCTION

Metal–organic frameworks (MOFs) have attracted tremendous attention as potential materials for gas storage, separation, luminescence, imaging, drug delivery, and heterogeneous catalysis in the last 2 decades.[1] Luminescent MOFs are of great interest because of their various applications in chemical sensing, photochemistry, and electroluminescent display. In addition, the tunable pore size, shape, and high surface of these materials permits the accommodation of guest molecules within their frameworks, offering another degree of tunability in their emission properties.[2] However, in order to get a wider range of applications, the stability of MOFs used as luminescent materials is crucial, especially their stability in air and water. So, it is a significant and challenging task to obtain stable MOFs for luminescent materials,[3] providing the conditions for further modification. Postsynthetic modification of MOFs has emerged as an effective tool for constructing functional MOFs with the encapsulation of Ln^{3+} ions. Recently, bio-MOF-1 and COMOC-4 have been used to generate a new class of luminescent Ln^{3+}@MOFs by the encapsulation of Ln^{3+} cations.[4] The encapsulation of Ln^{3+} ions not only offers a new platform to prepare Ln^{3+}-doped luminescent MOFs for tunable fluorescent materials but also provides a good opportunity to obtain Ln^{3+} probe materials for the detection of small molecules.

White-light-emitting-diode (WLED) materials have been extensively investigated in recent years because of their potential applications in backlights, lasers, indicators, and displays.[5,6] Currently, mercury-containing fluorescent lighting is one of the most widely used white-light sources, which rely on the emission of mercury vapor to excite semiconductor phosphors and to achieve white composite photoluminescence (PL).[7] However, the extensive use of mercury raises various environmental concerns. Thus, tremendous efforts have been dedicated to searching for more environmentally friendly, safer, and more energy-efficient white phosphor materials for use in the WLEDs.[8,9] MOF materials possess unique advantages for luminescence-based applications primarily because of their capability of incorporating light-emissive building blocks as both metal centers and organic ligands. This allows efficient modulation of the luminescent properties. It remains a great challenge to produce high-performance white-emitting MOF materials suitable for solid-state lighting applications. To date, only a few examples of direct white-light-emitting MOFs have been realized.[10] Doping the framework structures by rare metals (for example, Eu^{3+}, Tb^{3+}, and Dy^{3+}) at various concentrations may lead to white light.[11] However, most white-light-emitting

Received: December 9, 2014
Published: March 13, 2015

DOI: 10.1021/ic5029383
Inorg. Chem. 2015, 54, 3290–3296

MOF materials are unstable. Thus, it is very important and essential to obtain highly stable and efficient white-light-emitting MOF materials.

On the other hand, the fast, efficient, and reliable detection of explosives is of great significance for security screening, homeland security, environmental, and humanitarian implications.[12] Among various approaches for the detection of explosives, optical sensors show considerable advantages over others for their simplicity, convenience, and low cost of implementation, in which the sensing process is often accompanied by changes in the absorption and/or fluorescence spectra. Currently, some new molecular, polymeric, oligomeric, and nanoscale materials are often used for fluorescence detection. These materials can quickly, efficiently, and credibly detect various explosives,[13] but there are also some drawbacks, such as stability, toxicity, sensitivity, and biodegradability. In contrast, detection based on fluorescence quenching has advantages over other detection methods for its simplicity, short response time, high sensibility, and ability to be applied in both solution and solid phases.[14,15] In addition, the accessible porosity within MOF materials and the host−guest interactions will impart them with the capability of transducing the host−guest behavior to detectable changes; thus, porous MOFs are postulated as excellent candidates for chemical sensing applications.[16] Recently, a number of fluorescent MOFs showing explosive sensing have been reported.[17] However, Ln^{3+}-doped luminescent MOFs used for the detection of explosives have not been studied. For the first time, we developed a luminescent Ln^{3+}@MOF approach to realize the first Ln^{3+}@MOF sensor that can be used fast and effectively to detect nitroaromatic explosives with high recyclability through fluorescence quenching.

Given the above consideration, it is challenging to obtain dual-functional materials with high chemical stability that not only can be used to encapsulate Ln^{3+} ions for tunable fluorescent materials and white-light emission but also can detect explosives. The luminescent behavior of MOFs is highly dependent on the organic ligand. Hence, enhanced performance can be achieved by careful selection of the organic ligand. We selected carbazole-based ligand 9*H*-carbazole-3,6-dicarboxylic acid (H_2L) for the following reasons: (1) The carbazole group has a strong absorption in the short-wavelength range with a band gap of the energy level of about 3.2 eV and exhibits blue-light emission; thus, carbazole-based ligands are often used as luminescent materials. (2) The rigid carbazole group possesses strong electron-donating ability, with a condensed ring structure and good conjugates. Numerous explosives are good electron acceptors with an electron-deficient $-NO_2$ group, including the hazardous explosives nitrobenzene (NB), 2,6-dinitrotoluene (2,6-DNT), 1,3-dinitrobenzene (1,3-DNB), 2,4,6-trinitrotoluene (TNT), and 2,4,6-trinitrophenol (TNP), which are common chemical constituents of commercial explosives.[12c] The combination of the electron-donating H_2L and the electron-accepting $-NO_2$ group endow the compound with a prominent solvatochromic effect, which may be as fluorescent sensors to detect nitroaromatics.

Fortunately, a stable microporous MOF, $[Zn_4O(L)_3(H_2O)_2]_3$-$[Zn_4O(L)_3]\cdot x$DMF (NENU = Northeast Normal University; DMF = *N*,*N*-dimethylformamide), was synthesized. **NENU-522** was structurally characterized, and the luminescence of Ln^{3+}-loaded **NENU-522** was investigated. White-light emission was achieved by encapsulating different molar ratios of Eu^{3+} and Tb^{3+} ions into **NENU-522**. Furthermore, **Ln^{3+}@NENU-522** was employed as the sensor for the detection of nitro-containing compounds through fast and efficient fluorescence quenching.

EXPERIMENTAL SECTION

Materials and Methods. All chemical materials were obtained from commercial sources and used without further purification. 9*H*-Carbazole-3,6-dicarboxylic acid (H_2L) was synthesized by following the published method.[18] Fourier transform infrared (FT-IR) spectra were recorded in the range 4000−400 cm^{-1} on a Mattson Alpha-Centauri spectrophotometer using KBr pellets. Powder X-ray diffraction (PXRD) patterns were acquired on a Siemens D5005 diffractometer with Cu Kα (λ = 1.5418 Å) radiation in the range of θ = 3−50° at 293 K. Thermogravimetric analysis (TGA) was performed on a PerkinElmer TG-7 analyzer heated from room temperature to 800 °C at a ramp rate of 5 °C/min under a nitrogen gas atmosphere. Elemental analyses (C, H, and N) were conducted on a PerkinElmer 240C elemental analyzer. Zn and Ln were determined by inductively coupled plasma (ICP) analysis with a ICP-OES spectrometer (USA). Fluorescence spectra for the compounds were performed on an F-4600 FL spectrophotometer equipped with a Xe lamp and a quartz carrier at room temperature. When we investigated fluorescence spectra of **Ln^{3+}@NENU-522** in different concentrations of analyte molecules in DMF, the finely ground sample (3 mg) was immersed in 3 mL of the corresponding solution, treated by ultrasonication for 30 min, and then aged to form stable suspensions.

Synthesis of Compound NENU-522. H_2L (0.038 g, 0.15 mmol) and $Zn(NO_3)_2\cdot 6H_2O$ (0.0298 g, 0.1 mmol) were dissolved in DMF (5 mL). The mixture were sealed in a Teflon-lined stainless steel container and heated at 120 °C for 3 days, and then it was gradually cooled to room temperature, resulting in yellow crystals that were isolated by washing with DMF and dried at room temperature. Yield: 74% based on H_2L. Before the measurement, the sample was immersed in methanol for 72 h, and the extract was decanted. Fresh methanol was subsequently added, and the crystals were allowed to stay for an additional 24 h to remove the nonvolatile solvates. The sample was collected by decanting and treated with dichloromethane similarly to remove methanol solvates. After removal of dichloromethane by decanting, the sample was activated by drying under a dynamic vacuum at 90 °C overnight. Elem. microanal. of the activated sample. Calcd for $C_{168}H_{96}N_{12}O_{58}Zn_{16}$ (4256.49): C, 47.36; H, 2.25; N, 3.95. Found: C, 48.11; H, 2.01; N, 3.94.

Synthesis of Eu^{3+}/Tb^{3+}@NENU-522 Composites. **Eu^{3+}/Tb^{3+}@NENU-522** samples were prepared by immersing freshly prepared compound **NENU-522** in DMF solutions of lanthanide nitrates with molar ratios of 1:2, 1:1, and 2:1 (total amount: 0.06 mmol in 5 mL of DMF). After 2 days of soaking, the crystals were taken out of solution and washed with DMF to remove residual Ln cations on the surface. A similar process was employed to prepare a Eu^{3+}- or Tb^{3+}-doped sample by soaking a sample of **NENU-522** in DMF solutions of lanthanide nitrates of Eu^{3+} or Tb^{3+} (0.06 mmol in 5 mL of DMF). After 1 and 2 days of soaking, respectively, the crystals were washed with DMF to remove residual Ln cations on the surface.

X-ray Crystallography. Single-crystal X-ray diffraction data for compound **NENU-522** in this work were recorded on a Bruker APEXII CCD diffractometer with graphite-monochromated Mo Kα radiation (λ = 0.71069 Å) at 293 K. Absorption corrections were applied using a multiscan technique. The structure was solved by direct methods with *SHELXS-97*[19] and refined by full-matrix least-squares techniques using the *SHELXL-97* program[20] within *WINGX*.[21] Non-H atoms were refined with anisotropic temperature parameters. The *SQUEEZE* program implemented in *PLATON* was used to remove these electron densities for **NENU-522**. Thus, all of electron densities from free solvent molecules have been "squeezed" out. The detailed crystallographic data and structure refinement parameters for **NENU-522** are summarized in Table S1 in the Supporting Information (SI). CCDC 1025574 for **NENU-522** contains the supplementary crystallographic data for this paper. These data can be obtained free of charge from The Cambridge Crystallographic Data Centre.

DOI: 10.1021/ic5029383
Inorg. Chem. 2015, 54, 3290−3296

RESULTS AND DISCUSSION

Single-crystal X-ray diffraction analysis revealed that **NENU-522** crystallizes in the trigonal space group $R\bar{3}$. The asymmetric unit contains $^{4}/_{3}$ $Zn_4(\mu_4\text{-}O)$ cluster consisting of four Zn cations, one μ_4-O atom, and four deprotonated L^{2-} ligands. There are two kinds of $Zn_4(\mu_4\text{-}O)$ clusters in **NENU-522** (Figure S1 in the SI). The one $Zn_4(\mu_4\text{-}O)$ cluster is encapsulated by six carboxylate groups from six H_2L ligands to form a classic secondary building unit (SBU), $[Zn_4O(CO_2)_6]$, in IRMOF-*n*.[22] In **NENU-522**, Zn4 adopts six-coordinated octahedral geometry, while Zn1, Zn2, Zn3, Zn5, and Zn6 have tetrahedral coordination geometry, which is the same as that in a classic MOF (Figures S1 and S2 in the SI). The Zn_4O SBUs are connected by the six ligands to generate an interesting 3D microporous framework (Figure 1b). In the striking

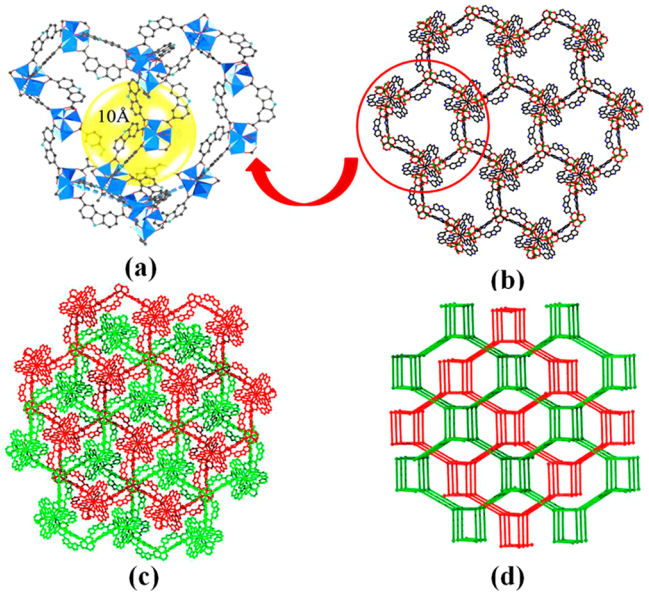

Figure 1. (a) Microporous cage in **NENU-522**. (b and c) Ball-and-stick representations of the 3D structure of **NENU-522**. (d) (10,3)-a topology network in **NENU-522**. All H atoms have been omitted for clarity.

structural feature of **NENU-522**, truncated cages delimited by 30 H_2L ligands and 14 Zn_4O SBUs. Using the central N atoms as the points of the cage, its diameter is about 1.0 nm (Figure 1a). Notably, there are two sets of such nets in **NENU-522**, and they interlock together to generate a 2-fold interpenetrating robust framework (Figure 1c). The overall structure of the compound is a 3D (10,3)-a network, in which the Zn_4O SBUs are regarded as 3-connected nodes (Figures 1d and S3 in the SI). The void space accounts for approximately 72.30% of the whole crystal volume as obtained by *PLATON* analysis.[23]

Good agreement between the calculated and experimental PXRD patterns verifies the purity of the as-synthesized sample. Moreover, under ambient conditions, **NENU-522** after exposure in air for more than 2 weeks was confirmed to be stable by agreement between the simulated and experimental PXRD patterns (Figure S4 in the SI). Surprisingly, it was also found that **NENU-522** exhibits outstanding chemical stability in acidic and basic aqueous solutions (HCl and NaOH, respectively) in the pH range of 4−12 (Figures S5 and S6 in the SI). Only a few MOFs that are stable in both acidic and basic solutions have been reported.[24] The thermal stability of **NENU-522** was examined using TGA in a dry nitrogen atmosphere. The first step from room temperature to 200 °C with ca. 35.9% weight loss is due to the loss of lattice DMF and water molecules, and then it begins to decompose upon further heating (Figure S10 in the SI). In addition, the PL spectra of H_2L and as-synthesized **NENU-522** samples in powder form were studied at room temperature. Under excitation at 320 nm, **NENU-522** exhibited significantly enhanced bright-blue-light emission with an emission maximum at 449 nm, which can be attributed to H_2L ligand-centered emission because a similar emission can be observed at 441 nm upon excitation at the same wavelength for the free H_2L ligand (Figure S7 in the SI). The Commission International de l'Eclairage (CIE) coordinates for the blue emission of **NENU-522** were calculated to be (0.1528, 0.1024), close to those of a saturated blue-light emitter with CIE coordinates of (0.14, 0.08).[25] The data demonstrate that **NENU-522** is an efficient blue-light emitter.

Because of the feature of the carbazole-based ligand, the porosity of **NENU-522** encouraged us to employ it as a host to encapsulate Ln^{3+} ions for the preparation of tunable fluorescent materials. In an initial attempt, through soaking of the freshly prepared samples in DMF solutions of nitrate salts of Ln^{3+} (0.2 mmol L^{-1}; Ln^{3+} = Sm^{3+}, Eu^{3+}, Tb^{3+}, or Dy^{3+}) for 24 h, Ln^{3+} ions were introduced into the channels of the framework. Then, the **Ln^{3+}@NENU-522** samples were filtered off, washed with DMF several times until no characteristic emission was observed upon excitation in a filtrate, and dried in air. Judging from the evidence of the IR spectra combined with the PXRD patterns, their basic frameworks are still retained (Figures S8 and S9 in the SI). The result is further analyzed by ICP and TGA curves, in which each unit cell of **NENU-522** can accommodate about 1.28 Ln^{3+} ions (Table S2 and Figure S10 in the SI). Here we studied the PL spectra of **Ln^{3+}@NENU-522** in the solid state in detail. **Sm^{3+}@NENU-522**, **Eu^{3+}@NENU-522**, and **Dy^{3+}@NENU-522** display very similar emissions but different

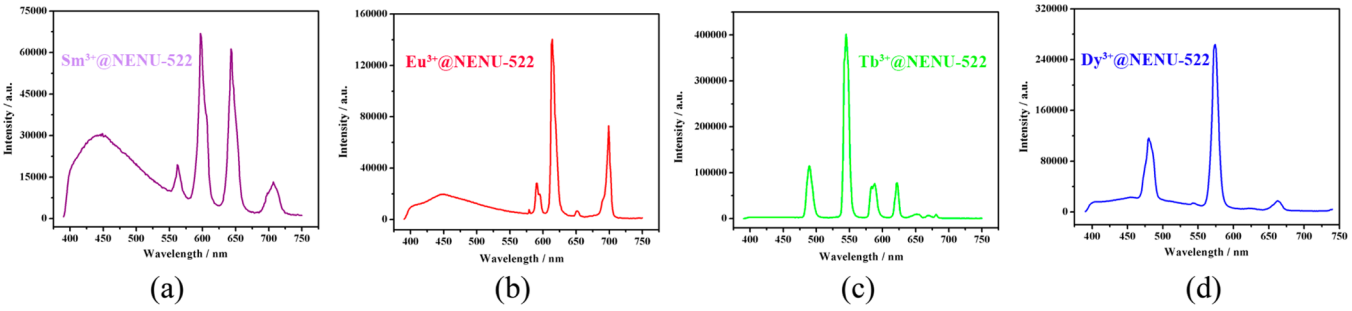

Figure 2. Emission spectra of (a) **Sm^{3+}@NENU-522**, (b) **Eu^{3+}@NENU-522**, (c) **Tb^{3+}@NENU-522**, and (d) **Dy^{3+}@NENU-522** (λ_{ex} = 333 nm).

DOI: 10.1021/ic5029383
Inorg. Chem. 2015, 54, 3290−3296

intensities, with the emission band at about 449 nm originating from **NUNU-522**. In addition, **Sm^{3+}@NENU-522** displays strong characteristic emissions at 562, 597, 643, and 707 nm, which can be assigned to the $^4G_{5/2} \rightarrow {}^6H_J$ ($J = {}^5/_2$, ${}^7/_2$, ${}^9/_2$, and ${}^{11}/_2$, respectively) emission transitions (Figure 2a). As for **Eu^{3+}@NENU-522**, a distinctive red color in the solid state at room temperature was clearly observed upon excitation at 333 nm. Five emission bands at 579, 591, 614, 652, and 699 nm correspond to the characteristic emission $^5D_0 \rightarrow {}^7F_J$ ($J = 0-4$) transitions (Figure 2b).[26] As for **Dy^{3+}@NENU-522**, emissions at 480, 574, and 662 nm were observed under excitation at 333 nm (Figure 2d), which can be assigned to the characteristic $^4F_{9/2} \rightarrow {}^6H_{15/2}$, $^4F_{9/2} \rightarrow {}^6H_{13/2}$, and $^4F_{9/2} \rightarrow {}^6H_{11/2}$ transitions of Dy^{3+}, respectively. Under the same conditions, it should be noted that the luminescence intensity of the highest characteristic peak of **Tb^{3+}@NENU-522** is much higher than that of **Ln^{3+}@NENU-522**. **Tb^{3+}@NENU-522** emits an intense green luminescence upon excitation at 333 nm, which is assigned to the characteristic transitions of $^5D_4 \rightarrow {}^7F_J$ ($J = 3-6$) of the Tb^{3+} ions.[27] Four emission bands at 489, 545, 588, and 622 nm originate from $^5D_4 \rightarrow {}^7F_6$, $^5D_4 \rightarrow {}^7F_5$, $^5D_4 \rightarrow {}^7F_4$, and $^5D_4 \rightarrow {}^7F_3$, respectively (Figure 2c). The above results prove that compound **NENU-522** is suitable for sensitization of the Ln^{3+} emitter; thus, it can serve as a host for encapsulating Ln^{3+} ions for tunable fluorescence emission. Moreover, the values of the corresponding CIE coordinates calculated are (0.3233, 0.2606) for **Sm^{3+}@NENU-522**, (0.3852, 0.2643) for **Eu^{3+}@NENU-522**, (0.3354, 0.5664) for **Tb^{3+}@NENU-522**, and (0.3301, 0.3742) for **Dy^{3+}@NENU-522** (Figure S11 in the SI). To some extent, the corresponding CIE coordinates for **Sm^{3+}@NENU-522** and **Dy^{3+}@NENU-522** approach the coordinates of white light; thus, we can say that near-white-light emission was achieved by the encapsulation of Sm^{3+} and Dy^{3+} ions.

To obtain pure white-light emission, rare-earth ions could emit pure visible lights; for example, red Eu^{3+} and green Tb^{3+} emissions have been commonly applied. In principle, if these two primary colors are further combined with blue luminescence, which is often contributed by the ligand-based emission, white-light emission can be realized. To evaluate their effects on **NENU-522**, the samples of Eu^{3+}- and Tb^{3+}-codoped **NENU-522** were prepared and their luminescent properties were studied. Under excitation at 320 nm, the corresponding CIE coordinates of **Eu^{3+}/Tb^{3+}@NENU-522** (1:1 and 2:1 Eu/Tb) are (0.2764, 0.2883) and (0.2752, 0.2708). The MOF emission color was fine-tuned to white by soaking **NENU-522** in DMF solutions containing nitrate salts of Eu^{3+} and Tb^{3+} ions in an optimal molar ratio of 1:2. The corresponding CIE coordinates for this sample is (0.2917, 0.3211), which is very close to that of the pure white light (0.33, 0.33). Figure 3 shows photographs of the white codoped samples excited by a standard laboratory ultraviolet (UV) lamp (365 nm). Moreover, the white-light-emitting **Eu^{3+}/Tb^{3+}@NENU-522** sample remains stable after exposure in air for more than 2 weeks (Figure S12 in the SI). We realized the adjustable preparation of the white material by encapsulating different molar ratios of red Eu^{3+} and green Tb^{3+} into the blue **NENU-522**.

In addition, the fluorescence properties of **NENU-522** in different solvent emulsions were also investigated (Figure S13 in the SI). The predominant feature is that the PL intensities are largely dependent on the solvent molecules, particularly in the case of NB, which exhibits significant quenching behavior. The physical interaction of the solute and solvent acts a vital

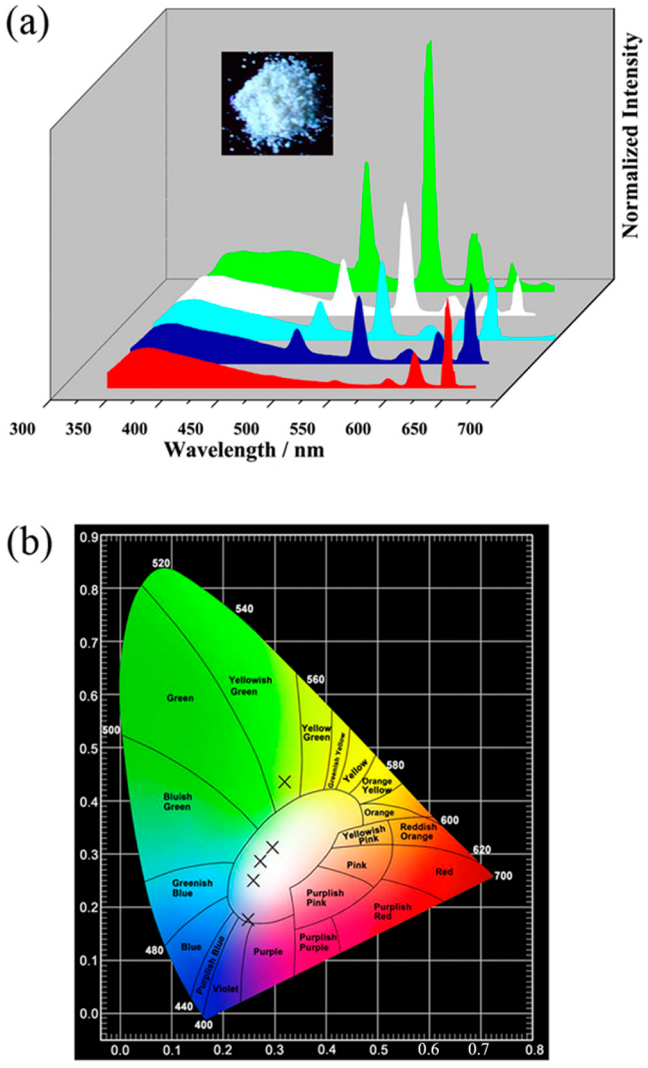

Figure 3. (a) Emission spectra of **Eu^{3+}@NENU-522** (red), **Tb^{3+}@NENU-522** (green), and **Eu^{3+}/Tb^{3+}@NENU-522** [1:2 (white), 1:1 (turquiose), and 2:1 (blue) Eu/Tb] excited at 320 nm. Inset: Photograph of the white-light-emitting **Eu^{3+}/Tb^{3+}@NENU-522** (1:2 Eu/Tb) excited under a 365 nm UV lamp. (b) Corresponding chromaticity coordinates of these samples: CIE = (0.2434, 0.1792), (0.3145, 0.4307), (0.2917, 0.3211), (0.2764, 0.2883), and (0.2752, 0.2708).

role in such fluorescence behavior. Luminescence quenching is related to the electron-withdrawing $-NO_2$ group, and all Ln^{3+} ions except La^{3+} and Lu^{3+} can generate luminescent f−f emissions from UV to visible and near-infrared ranges. Sm^{3+}, Eu^{3+}, Tb^{3+}, and Dy^{3+} emit orange, red, green, and blue light upon adequate excitation, respectively, which are easy to observe. We use **Tb^{3+}@NENU-522** to detect nitroaromatic explosives, taking that the luminescence intensity of **Tb^{3+}@NENU-522** is much higher than that of **Ln^{3+}@NENU-522**. The fluorescence detection experiments of **Tb^{3+}@NENU-522** were performed to examine the sensing sensitivity to a series of nitroaromatic explosives such as NB, 1,3-DNB, TNP, and so on. To examine the sensing sensitivity toward TNP in more detail, a batch of suspensions of **Tb^{3+}@NENU-522** were prepared by dispersing it in a DMF solution while gradually increasing the contents to monitor the emissive response. The luminescence intensity has decreased 35% only at 5 ppm and 58% at 10 ppm, and complete quenching occurred at 80 ppm

DOI: 10.1021/ic5029383
Inorg. Chem. 2015, 54, 3290−3296

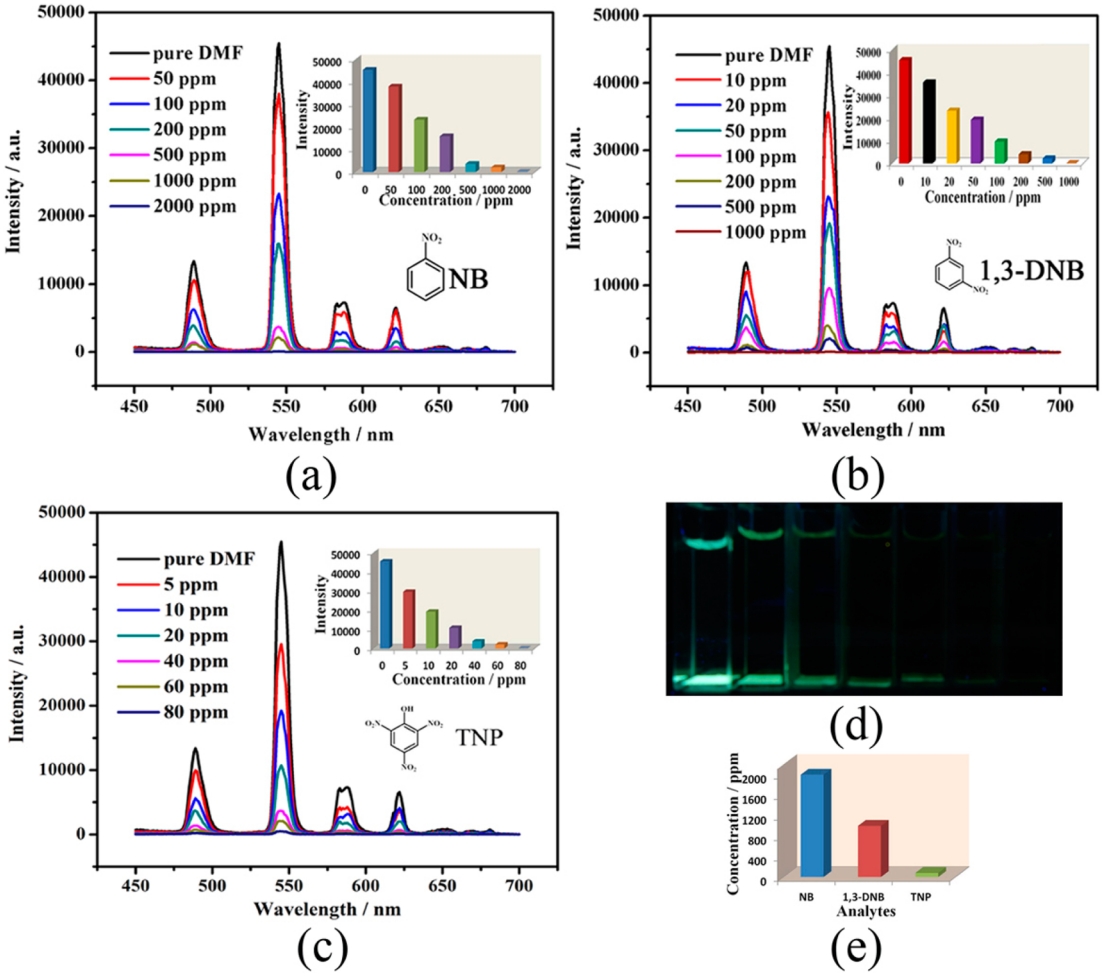

Figure 4. (a–c) Emission spectra of **Tb^{3+}@NENU-522** in different concentrations of NB, 1,3-DNB, and TNP in DMF (excited at 333 nm), respectively. Inset: Corresponding emission intensities. (d) Photograph showing the procedure of fluorescence quenching upon the addition of TNP under UV light (365 nm). (d) Corresponding emission intensities of **Tb^{3+}@NENU-522** in different concentrations of TNP in DMF. (e) Contrast of the lowest concentrations of complete quenching for NB, 1,3-DNB, and TNP.

(Figures 4c,d and S14 in the SI). The finely ground powders could be dispersed well in the analyte solutions, which enables nitro-containing compounds to be closely adhered to the surface of **Tb^{3+}@NENU-522** particles, facilitating probable host–guest interaction. Here, electron transfer from a electron-donating framework to high electron deficiency can take place upon excitation, causing fluorescence quenching. Similar quenching phenomena were reported in the previous works.[28] Similar fluorescence quenching is recorded by the PL spectra (λ_{ex} = 333 nm) when the NB and 1,3-DNB molecules are added to DMF. The fluorescence intensities decrease with an increase of the concentration of the analytes added to DMF. The luminescence intensities have decreased 47% of the original intensity at 100 ppm for NB and 49% at 20 ppm for 1,3-DNB. The lowest concentrations of complete quenching are 2000 ppm for NB and 1000 ppm for 1,3-DNB (Figures 4a,b and S15 and S16 in the SI). The results indicate that **Tb^{3+}@NENU-522** displays the most effective detection for TNP (Figure 4e). In other words, the lowest concentrations of complete quenching decrease with an increase in the number of $-NO_2$ of nitroaromatic explosives. These explosives are electron acceptors with electron-deficient $-NO_2$ groups, and the skeleton of **NENU-522** possesses strong electron-donating ability with rigid carbazole groups. So, we conclude that, with increasing $-NO_2$ groups, energy transfer from the electron-donating framework to high electron deficiency becomes more, making the effect of fluorescence quenching more obvious.

To further demonstrate the phenomena, we also investigated the potential of **Tb^{3+}@NENU-522** toward sensing 2,6-DNT and TNT. The luminescence intensities have decreased 54% at 100 ppm for 2,6-DNT and 45% at 10 ppm for TNT. The lowest concentrations of complete quenching are 1000 ppm for 2,6-DNT (Figures S17 and S18 in the SI) and 100 ppm for TNT (Figure S19 and S20 in the SI), and the results are consistent with our expectation. The relationships between the emission intensity and different concentrations of analytes indicate that **Tb^{3+}@NENU-522** displays the most effective detection for TNP and TNT containing three $-NO_2$ groups (Figure S21 in the SI). What is more, the complete quenching concentration of nitro-containing compounds (NB, 1,3-DNB, 2,6-DNT, TNT, and TNP) and the number of $-NO_2$ groups demonstrated good linear relationships (Figure S22 in the SI). The color of the dispersed solution of **Tb^{3+}@NENU-522** powders under a UV lamp totally disappeared upon the addition of an analyte solution (Figure 4d). Therefore, we can highly detect these nitro-containing compounds only by the color change, which is extremely convenient and fast. The lowest concentrations of complete quenching are about 2000 ppm for

DOI: 10.1021/ic5029383
Inorg. Chem. 2015, 54, 3290–3296

NB with one $-NO_2$ group, 1000 ppm for 1,3-DNB and 2,6-DNT with two $-NO_2$ groups, and 80 and 100 ppm for TNP and TNT with three $-NO_2$ groups. **Tb^{3+}@NENU-522** is found to be useful as a fluorescent indicator for the qualitative and quantitative detection of nitroaromatic explosives with different numbers of $-NO_2$ groups. In particular, **Tb^{3+}@NENU-522** can be regenerated for recycling to detect these nitro-containing compounds by centrifuging the solution after use and washing several times with DMF. The quenching efficiencies of cycles 1−6 are basically unchanged above 90%, displaying high recyclability and stability in the detection application (Figures 5 and S23 in the SI). The framework can still remain after the detection of different analytes, as confirmed by PXRD and FT-IR (Figures S24 and S25 in the SI).

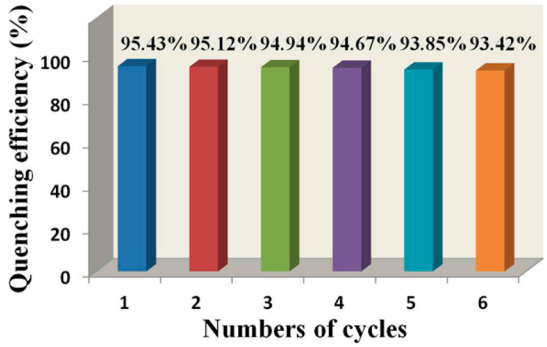

Figure 5. Quenching efficiency of **Tb^{3+}@NENU-522** dispersed in DMF to 60 ppm in a TNP solution by centrifuging the solution after use and washing several times with DMF.

CONCLUSIONS

In summary, we have synthesized a luminescent MOF material constructed from Zn_4O clusters, which is extremely stable in air and acidic/basic aqueous solutions at room temperature. It can serve as a host for the encapsulation of Ln^{3+} ions to obtain tunable luminescent emission. White-light emission was achieved by encapsulating Eu^{3+} and Tb^{3+} (1:2 Eu/Tb) into **NENU-522**. For the first time, we developed a luminescent Ln^{3+}@MOF approach to realize a fast and effective Ln^{3+}@MOF sensor used to detect nitroaromatic explosives with high recyclability through fluorescence quenching. The concentrations of complete quenching are about 2000, 1000, and 80 ppm for NB, 1,3-DNB, and TNP with different numbers of $-NO_2$ groups, respectively. The study provides a promising example of dual-functional materials with high chemical stability to encapsulate Ln^{3+} ions for white-light emission and to detect nitroaromatic explosives. The present work provides a promising approach to the design of MOF-based white-light-emission materials and explosive sensors, which are probably useful in more realistic conditions in the future.

ASSOCIATED CONTENT

Supporting Information

PXRD patterns, TGA curves, IR and PL spectra, additional figures, and crystallographic data (CIF). This material is available free of charge via the Internet at http://pubs.acs.org.

AUTHOR INFORMATION

Corresponding Authors

*E-mail: zmsu@nenu.edu.cn.
*E-mail: fuq836@nenu.edu.cn.
*E-mail: yqlan@njnu.edu.cn.

Notes

The authors declare no competing financial interest.

ACKNOWLEDGMENTS

This work was financially supported by the Pre-973 Program (Grant 2010CB635114), the National Natural Science Foundation of China (Grants 21371099 and 21471080), the Science and Technology Development Planning of Jilin Province (Grant 20140203006GX), the Jiangsu Specially-Appointed Professor, the NSF of Jiangsu Province of China (Grant BK20130043), the Natural Science Research of Jiangsu Higher Education Institutions of China (Grant 13KJB150021), the Priority Academic Program Development of Jiangsu Higher Education Institutions, and the Foundation of Jiangsu Collaborative Innovation Center of Biomedical Functional Materials.

REFERENCES

(1) (a) Kim, K. *Nat. Chem.* **2009**, *1*, 603−604. (b) Ferey, G. *Chem. Soc. Rev.* **2008**, *37*, 191−214. (c) Yaghi, O. M. *Nat. Mater.* **2007**, *6*, 92−93. (d) Toh, N. L.; Nagarithinum, N.; Vittal, J. J. *Angew. Chem., Int. Ed.* **2005**, *44*, 2237−2241. (e) Pan, L.; Liu, H.; Lei, X.; Huang, X.; Olson, D. H.; Turro, N.; Li, J. *Angew. Chem., Int. Ed.* **2003**, *42*, 542−546. (f) Murray, L. J.; Dinca, M.; Long, J. R. *Chem. Soc. Rev.* **2009**, *38*, 1294−1314. (g) Xu, X.; Nieuwenhuyzen, M.; James, S. L. *Angew. Chem., Int. Ed.* **2002**, *41*, 764−767. (h) Chakrabarty, R.; Mukherjee, P. S.; Stang, P. J. *Chem. Rev.* **2011**, *111*, 6810−6918. (i) Allendorf, M. D.; Bauer, C. A.; Bhakta, R. K.; Houk, R. J. T. *Chem. Soc. Rev.* **2009**, *38*, 1330−1352.

(2) (a) Cui, Y.-J.; Yue, Y.-F.; Qian, G.-D.; Chen, B.-L. *Chem. Rev.* **2012**, *112*, 1126−1162. (b) Cui, Y.-J.; Xu, H.; Yue, Y.-F.; Guo, Z.-Y.; Qian, G.-D.; Chen, B.-L. *J. Am. Chem. Soc.* **2012**, *134*, 3979−3982. (c) Sun, C.-Y.; Wang, X.-L.; Zhang, X.; Qin, C.; Li, P.; Su, Z.-M.; Li, J. *Nat. Commun.* **2013**, *4*, 2717−2724.

(3) (a) Chen, Y.-Q.; Li, G.-R.; Chang, Z.; Qu, Y.-K.; Zhang, Y.-H.; Bu, X.-H. *Chem. Sci.* **2013**, *4*, 3678−3682. (b) Liao, J.-H.; Chen, W.-T.; Tsai, C. S.; Wang, C.-C. *CrystEngComm* **2013**, *15*, 3377−3384.

(4) (a) An, J. Y.; Shade, C. M.; Chengelis-Czegan, D. A.; Petoud, S.; Rosi, N. L. *J. Am. Chem. Soc.* **2011**, *133*, 1220−1223. (b) Liu, Y.-Y.; Decadt, R.; Bogaerts, T.; Hemelsoet, K.; Kaczmarek, A. M.; Poelman, D.; Waroquier, M.; Van Speybroeck, V.; Van Deun, R.; Van Der Voort, P. *J. Phys. Chem. C* **2013**, *117*, 11302−11310.

(5) (a) Reineke, S.; Lindner, F.; Schwartz, G.; Seidler, N.; Walzer, K.; Luessem, B.; Leo, K. *Nature* **2009**, *459*, 234−238. (b) Xiao, L.; Chen, Z.; Qu, B.; Luo, J.; Kong, S.; Gong, Q.; Kido, J. *Adv. Mater.* **2011**, *23*, 926−952. (c) Fleetham, T.; Ecton, J.; Wang, Z.; Bakken, N.; Li, J. *Adv. Mater.* **2013**, *25*, 2573−2576.

(6) (a) Wang, Q.; Ma, D.-G. *Chem. Soc. Rev.* **2010**, *39*, 2387−2398. (b) Jang, H.-S.; Yang, H.; Kim, S. W.; Han, J.-Y.; Lee, S. G.; Jeon, D. Y. *Adv. Mater.* **2008**, *20*, 2696−2702. (c) Jang, E.; Jun, S.; Jang, H.; Lim, J.; Kim, B.; Kim, Y. *Adv. Mater.* **2010**, *22*, 3076−3080. (d) Nicolai, H. T.; Hof, A.; Blom, P. W. M. *Adv. Funct. Mater.* **2012**, *22*, 2040−2047. (e) Li, Y.; Xu, G.; Zou, W.-Q.; Wang, M.-S.; Zheng, F.-K.; Wu, M.-F.; Zeng, H.-Y.; Guo, G.-C.; Huang, J.-S. *Inorg. Chem.* **2008**, *47*, 7945−7947.

(7) Furman, J. D.; Warner, A. Y.; Teat, S. J.; Mikhailovsky, A. A.; Cheetham, A. K. *Chem. Mater.* **2010**, *22*, 2255−2260.

(8) (a) Green, W. H.; Le, K. P.; Grey, J.; Au, T. T.; Sailor, M. J. *Science* **1997**, *276*, 1826−1828. (b) Ki, W.; Li, J. *J. Am. Chem. Soc.* **2008**, *130*, 8114−8115. (c) Wada, Y.; Sato, M.; Tsukahara, Y. *Angew. Chem., Int. Ed.* **2006**, *45*, 1925−1928. (d) Zhao, Y.-S.; Fu, H.; Hu, F.; Peng, A.; Yang, W.; Yao, J. *Adv. Mater.* **2008**, *20*, 79−83.

(9) (a) Uchino, T.; Yamada, T. *Appl. Phys. Lett.* **2004**, *85*, 1164−1166. (b) Coppo, P.; Duati, M.; Kozhevnikov, V. N.; Hofstraat, J. W.; De Cola, L. *Angew. Chem., Int. Ed.* **2005**, *44*, 1806−1810. (c) Ki, W.;

DOI: 10.1021/ic5029383
Inorg. Chem. 2015, 54, 3290−3296

Li, J.; Eda, G.; Chhowalla, M. *J. Mater. Chem.* **2010**, *20*, 10676−10679. (d) Fang, X.-M.; Roushan, M.; Zhang, R.-B.; Peng, J.; Zeng, H.-P.; Li, J. *Chem. Mater.* **2012**, *24*, 1710−1717.
(10) (a) Wang, M.-S.; Guo, S.-P.; Li, Y.; Guo, G.-C. *J. Am. Chem. Soc.* **2009**, *131*, 13572−13573. (b) Wang, M.-S.; Guo, G.-C.; Chen, W.-T.; Xu, G.; Zhou, W.-W.; Wu, K.-J.; Huang, J.-S. *Angew. Chem., Int. Ed.* **2007**, *46*, 3909−3911. (c) Sava, D. F.; Rohwer, L. E.; Rodriguez, M. A.; Nenoff, T. M. *J. Am. Chem. Soc.* **2012**, *134*, 3983−3986. (d) He, J.; Zeller, M.; Hunter, A. D.; Xu, Z. T. *J. Am. Chem. Soc.* **2012**, *134*, 1553−1559.
(11) (a) Rao, X.-T.; Huang, Q.; Yang, X.-L.; Cui, Y.-J.; Yang, Y.; Wu, C.-D.; Chen, B.-L.; Qian, G.-D. *J. Mater. Chem.* **2012**, *22*, 3210−3214. (b) Huang, Y.-T.; Lai, Y.-C.; Wang, S.-L. *Chem.—Eur. J.* **2012**, *18*, 8614−8616. (c) Li, S.-M.; Zheng, X.-J.; Yuan, D.-Q.; Ablet, A.; Jin, L.-P. *Inorg. Chem.* **2012**, *51*, 1201−1203. (d) Liu, K.; You, H.-P.; Zheng, Y.-H.; Jia, G.; Zhang, H.-J. *Cryst. Growth Des.* **2010**, *10*, 16−19.
(12) (a) McQuade, D. T.; Pullen, A. E.; Swager, T. M. *Chem. Rev.* **2000**, *100*, 2537−2574. (b) Toal, S. J.; Trogler, W. C. *J. Mater. Chem.* **2006**, *16*, 2871−2883. (c) Germain, M. E.; Knapp, M. J. *Chem. Soc. Rev.* **2009**, *38*, 2543−2555.
(13) (a) Salinas, Y.; Martínez-Máñez, R.; Marcos, M. D.; Sancenón, F.; Costero, A. M.; Parraad, M.; Gil, S. *Chem. Soc. Rev.* **2012**, *41*, 1261−1296. (b) Thomas, S. W., III; Joly, G. D.; Swager, T. M. *Chem. Rev.* **2007**, *107*, 1339−1386. (c) Wang, Y.; La, A.; Ding, Y.; Liu, Y. X.; Lei, Y. *Adv. Funct. Mater.* **2012**, *22*, 3547−3555. (d) Naddo, T.; Che, Y. K.; Zhang, W.; Balakrishnan, K.; Yang, X. M.; Yen, M.; Zhao, J. C.; Moore, J. S.; Zang, L. *J. Am. Chem. Soc.* **2007**, *129*, 6978−6979. (e) Andrew, T. L.; Swager, T. M. *J. Am. Chem. Soc.* **2007**, *129*, 7254−7255. (f) Li, D.-D.; Liu, J.-Z.; Kwok, R. T. K.; Liang, Z.-Q.; Tang, B.-Z.; Yu, J.-H. *Chem. Commun.* **2012**, *48*, 7167−7169. (g) Shan, G.-G.; Li, H.-B.; Sun, H.-Z.; Zhu, D.-X.; Cao, H.-T.; Su, Z.-M. *J. Mater. Chem. C* **2013**, *1*, 1440−1449. (h) Tao, Y.; Li, G. T.; Zhu, H. S. *J. Mater. Chem.* **2006**, *16*, 4521−4528.
(14) Nagarkar, S. S.; Joarder, B.; Chaudhari, A. K.; Mukherjee, S.; Ghosh, S. K. *Angew. Chem., Int. Ed.* **2013**, *52*, 2881−2885.
(15) (a) Ghosh, S.; Mukherjee, P. S. *Organometallics* **2008**, *27*, 316−319. (b) Zyryanov, G. V.; Palacios, M. A.; Anzenbacher, P. *Org. Lett.* **2008**, *10*, 3681−3684. (c) Muthu, S.; Ni, Z.; Vittal, J. J. *Inorg. Chim. Acta* **2005**, *358*, 595−605. (d) Gole, B.; Shanmugamraju, S.; Bar, A. K.; Mukherjee, P. S. *Chem. Commun.* **2011**, *47*, 10046−10048.
(16) (a) Hu, Z.-C.; Deibert, B.-J.; Li, J. *Chem. Soc. Rev.* **2014**, *43*, 5815−5840. (b) Lan, A.; Li, K.; Wu, H.; Olson, D. H.; Emge, T. J.; Ki, W.; Hong, M. C.; Li, J. *Angew. Chem., Int. Ed.* **2009**, *48*, 2334−2338. (c) Harbuzaru, B. V.; Corma, A.; Rey, F.; Atienzar, P.; Jorda, J. L.; Garcia, H.; Ananias, D.; Carlos, L. D.; Rocha, J. *Angew. Chem., Int. Ed.* **2008**, *47*, 1080−1083.
(17) (a) Zhang, C.; Che, Y.; Zhang, Z.; Yang, X.; Zang, L. *Chem. Commun.* **2011**, *47*, 2336−2338. (b) Zhang, Z.-J.; Xiang, S.-C.; Rao, X.-T.; Zheng, Q.; Fronczek, F.-R.; Qian, G.-D.; Chen, B.-L. *Chem. Commun.* **2010**, *46*, 7205−7207. (c) Pramanik, S.; Zheng, C.; Zhang, X.; Emge, T. J.; Li, J. *J. Am. Chem. Soc.* **2011**, *133*, 4153−4155.
(18) Li, J.-R.; Timmons, D. J.; Zhou, H.-C. *J. Am. Chem. Soc.* **2009**, *131*, 6368−6369.
(19) Sheldrick, G. M. *SHELXS-97, Programs for X-ray Crystal Structure Solution*; University of Göttingen: Göttingen, Germany, 1997.
(20) Sheldrick, G. M. *SHELXL-97, Programs for X-ray Crystal Structure Refinement*; University of Göttingen: Göttingen, Germany, 1997.
(21) Farrugia, L. J. *WINGX, A Windows Program for Crystal Structure Analysis*; University of Glasgow: Glasgow, U.K., 1988.
(22) Zhao, D.; Timmons, D. J.; Yuan, D.-Q.; Zhou, H.-C. *Acc. Chem. Res.* **2011**, *44*, 123−133.
(23) (a) van der Sluis, P.; Spek, A. L. *Acta Crystallogr., Sect. A: Found. Crystallogr.* **1990**, *46*, 194−201. (b) Spek, A. L. *PLATON, A multipurpose crystallographic tool*; Utrecht University: Utrecht, The Netherlands, 2001.
(24) (a) Jiang, H.-L.; Feng, D.-W.; Wang, K.-C.; Gu, Z.-Y.; Wei, Z.-W.; Chen, Y.-P.; Zhou, H.-C. *J. Am. Chem. Soc.* **2013**, *135*, 13934−13938. (b) Yin, Z.; Wang, Q. X.; Zeng, M. H. *J. Am. Chem. Soc.* **2012**, *134*, 4857−4863.
(25) Wang, L.; Jiang, Y.; Luo, J.; Zhou, Y.; Zhou, J.; Wang, J.; Pei, J.; Cao, Y. *Adv. Mater.* **2009**, *21*, 4854−4858.
(26) (a) Qin, J.-S.; Du, D.-Y.; Chen, L.; Sun, C.-Y.; Lan, Y.-Q.; Su, Z.-M. *J. Solid State Chem.* **2011**, *184*, 373−378. (b) Sun, Y.-Q.; Zhang, J.; Chen, Y.-M.; Yang, G.-Y. *Angew. Chem., Int. Ed.* **2005**, *44*, 5814−5817.
(27) Sun, L.; Li, Y.; Liang, Z.-Q.; Yu, J.; Xu, R.-R. *Dalton Trans.* **2012**, *41*, 12790−12796.
(28) Wang, G.-Y.; Yang, L.-L.; Li, Y.; Song, H.; Ruan, W. J.; Chang, Z.; Bu, X. H. *Dalton Trans.* **2013**, *42*, 12865−12868.

DOI: 10.1021/ic5029383
Inorg. Chem. 2015, 54, 3290−3296